

FEDSM-ICNMM2010-' % \$*

FREQUENCY RESPONSE OF GAS-FILLED TUBE WITH MINOR LOSSES

Brian M. West

MAE Department
Utah State University
Logan, Utah, 84322

Email: brian.west@aggiemail.usu.edu

Barton L. Smith

MAE Department
Utah State University
Logan, Utah 84322

Email: barton.smith@usu.edu

Fei Liu

MAE Department
University of Florida
P.O. Box 116250
Gainesville, FL 32611-6250

Email: feicq@ufl.edu

Lou Cattafesta

MAE Department
University of Florida
P.O. Box 116250
Gainesville, FL 32611-6250

Email: cattafes@ufl.edu

Abstract

The results of a study of the frequency response of a pneumatic system designed to provide pulsed flow for flow control applications are presented. The system consists of a high pressure air source, a high-frequency solenoid valve, a length of tube and a minor loss. The experiment mimics the pneumatic drive for our Coanda-Assisted Spray Manipulation actuator and applies to many flow control applications involving pulsed flow. Square wave signals of various frequency were fed to the solenoid valve. The flow at the exit of the flow system was measured with a single hot wire and compared to steady flow through the same geometry. The effect of the inlet pressure, tube length and the size and position of the minor loss were tested. These data are modeled using a Transmission Matrix Model in

1 Introduction

Gas flowing in tubes driven by solenoid valves are used in many control systems. A solenoid valve is an electromechanical device that opens to allow fluid flow when an electrical signal is provided. Typically, a solenoid valve is “binary,” meaning that it is open or closed. The frequency response of a solenoid system is a complex function of the components, fluid properties, and operating conditions. Various factors affect the response, such as supply pressure, tube length, and minor losses, but there has been little research on the specific effects of these parameters on the overall response.

Research has been done on the flow inside solenoid valves by Szente and Vad [1]. Their experiments used semi-empirical models to predict loss coefficients through a valve with a Borda-type orifice given the seat angle of the valve. A Borda-type orifice is an orifice with an entrance

region that extends upstream in the flow. The seat angle interface between the Borda-type orifice and the valve seal varies. However, their interest was how the seat angle in the valve affected the magnitude of the minor loss through the valve, and the effect that this minor loss on the frequency response at the exit was not presented.

Braud *et al.* [2] showed that velocities up to two times higher than the steady state velocity through the same tubes can be obtained when pressure pulses are applied. The effect of waves traveling in the tube were modeled, including their effect on the settling time. They presented a model for the flow at the exit of a gas filled tube in both the continuous and transient cases, but the effects of pressure, and frequency were not presented, and their tube did not have minor losses near its termination. In the current experiment, the effects of the characteristics of the tube are studied further with minor losses on each end.

Oscillating gas flow in a tube is known to act analogously to a spring-mass-damper or electrical system. This system can be modeled as an equivalent electrical circuit composed of resistors, an inductor, and capacitor in series provided the device dimensions are small compared to the acoustic wavelength. The air between the two ends behaves as a mass, moving back and forth in response to a forcing function. The air also acts as a spring as it compresses and expands due to a changes in pressure. Viscous friction damps the system. At low frequencies, the system is well described by an electrical circuit consisting of an in line resistor, an inductor in line, and a capacitor and resistor in parallel going to ground [3]. The volume flow rate of the gas is analogous to current, and pressure is analogous to voltage. This circuit is shown in Fig. 1.

The compressibility of the gas is analogous to a capacitance, and is described by the equation $C = \frac{V}{\gamma p}$ where V is the volume of the gas, γ is the ratio of specific heats, and p is pressure. The inertia of the gas is analogous to inductance, described by $L = \frac{\rho \Delta x}{A}$ where ρ is the gas density, Δx is the length of tube, and A is the cross sectional area [3]. The frequency response of this system is of particular interest in determining limits to control systems. In the experiment presented, however, the flow is not oscillatory. It is pulsed or steady flow, but the principles of the circuit in Fig. 1 still help predict the behavior of gas flowing through a tube.

The present experiments investigate the variation of magnitude response and wave shape for a gas filled tube as a function of frequency, mean input pressure, tube length,

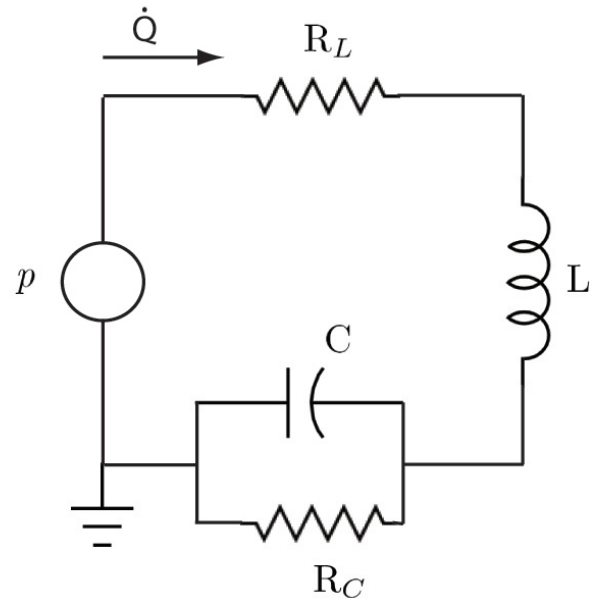


Figure 1. Theoretical circuit for a gas filled tube. Compressibility is represented by the capacitor, momentum by the inductor, and losses by the resistances. R_C is associated with losses in the capacitor and R_L is associated with losses in the inductor. Volume flow rate is the mechanical equivalent to current and p is the equivalent to voltage.

and minor loss

$$K_L = \frac{\Delta p}{\rho_0 U^2 / 2}, \quad (1)$$

and will help provide limits for control systems. The experimental facility and measurements will be described followed by results and conclusions.

2 Experimental Facility

A picture of the test setup is shown in Fig. 2. Compressed air was supplied to a pressure regulator which was controlled using an analog signal from a DAQ board from National Instruments and LabVIEW software. A pressure transducer from Omega was placed at the output of the pressure regulator and its analog output was sampled using the same board. The software set the time-averaged pressure to the desired value. The air was then fed through 5/32-inch inner diameter tubes into a solenoid valve from FESTO. Another tube connects the valve to a block containing a high-speed pressure sensor and a flow passage of

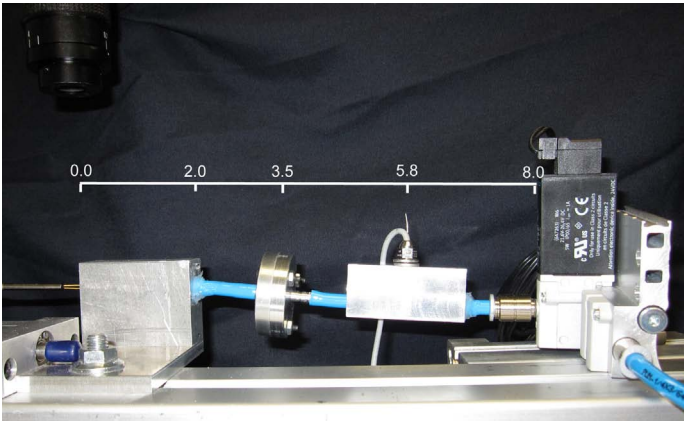


Figure 2. Experimental setup for a system with 3.5 inches of tube length. Dimensions are given in inches. The probe is positioned at the exit plane using a camera with microscope optics above the exit. The 2-inch exit block holds the tube to allow a hot film probe to be safely placed at the exit. The minor loss holder is located at 3.5 inches, and the pressure sensor is at 5.8 inches. The solenoid valve is at the right hand side of the image. For longer tube lengths, the tube between the minor loss and the exit block is changed.

the same ID as the tube to the variable minor loss. The length of the tube between the valve and minor loss was varied.

The hot film probe was connected to a constant temperature anemometer from TSI and its output was read by the DAQ board. The probe was calibrated using a calibration unit on site. Air properties were measured at calibration time and velocities were calculated using Bernoulli's equation. A curve fit was applied to compute the velocity from the hot film voltage.

The voltage to the solenoid valve was controlled by a solid state relay, model number HFS33, driven by the DAQ board. Square waves of various frequencies were sent through the relay to create pulses in the gas-filled tube.

In all cases, the frequency response is compared to steady flow through the same system. Sonic flow is suspected at points in the tube for some operating conditions, and choking through the minor loss is probable, especially in the cases with the highest loss. Steady flow was measured at various source pressures to observe general trends in the behavior of the average velocity, U (the velocity values are divided by 2 to allow comparison to a square wave as described below). In Fig. 3 the trend in the data appears to follow a power law and looks similar to the data of [2].

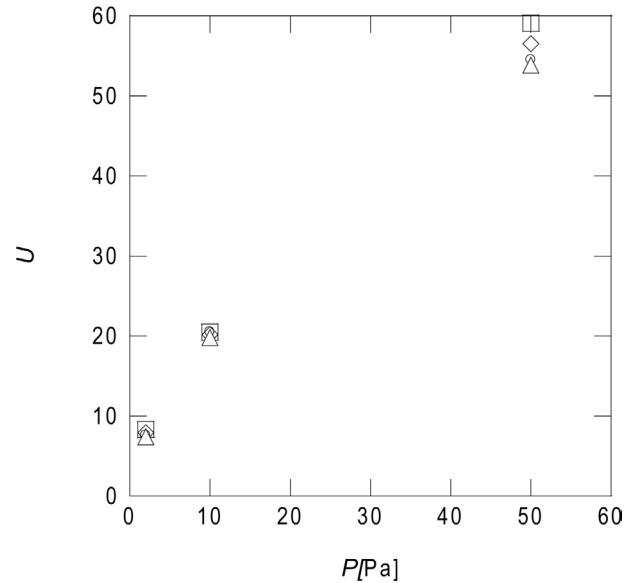


Figure 3. Graph showing a power law trend between pressure and standard deviation of velocity with a loss factor value of $K_L = 1.135$. $L = 1$ in (\circ), $L = 10$ in (\square), $L = 30$ in (\diamond), $L = 100$ in (\triangle)

This was the case for all but the largest K_L value, which is shown in Fig. 4. It is believed that the change in behavior is due to choking. The pressure does not scale with ρU^2 in most cases, which is likely due to compressible effects. With the pressure regulator available to us, the lowest supply pressure we could maintain was 2 psig, and even for lower pressures the relation did not help in normalizing steady state velocities.

The minor loss was varied by placing disks with different sized sharp-edged holes drilled through their center inside an orifice holder. Losses were modeled as a sudden contraction and a sudden expansion. Losses were computed for an expansion using $K_L = \alpha(1 - d^2/D^2)$ [4]. Values for K_L for a sudden contraction were taken from [4]. A sketch of the orifice holder is shown in Fig. 5.

The solenoid valve was driven by a 50% duty cycle square wave at various frequencies. Sampling rates were varied to provide independent samples and to capture a fixed number of periods for each non-steady case. All cases captured 10,000 data points. Rates and sampling times are given in Table 1. Parameters varied in the experiment are shown in Table 3.

The solid state relay was checked to determine its influence on the response. The signal from the DAQ board

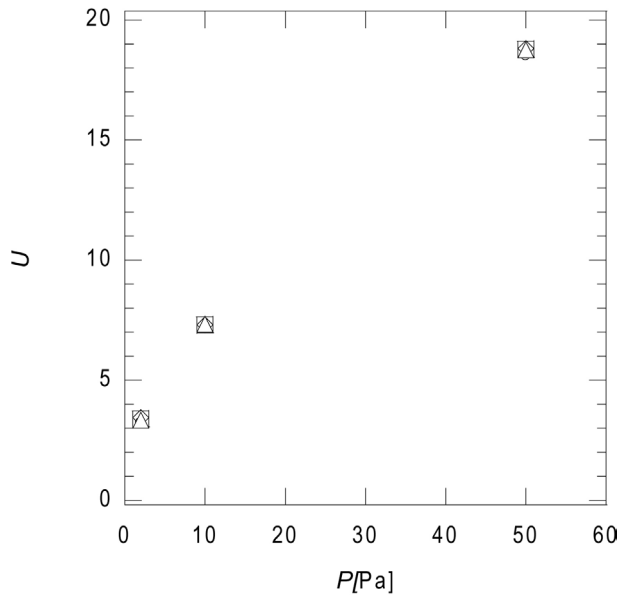


Figure 4. Steady flow velocity (divided by 2) as a function of source pressure for a minor loss value of 1.454. $L = 1in$ (\circ), $L = 10in$ (\square), $L = 30in$ (\diamond), $L = 100in$ (\triangle)

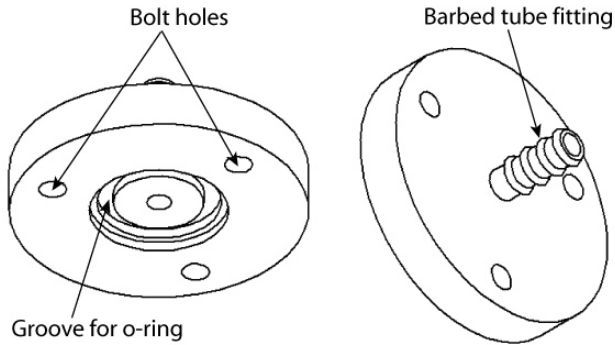


Figure 5. Minor loss element. Discs with varying center holes are held between the two pieces to create a sudden contraction and expansion.

Table 1. Sampling Parameters

Signal Frequency	Sampling Frequency	Sampling Period
f [Hz]	f_s [Hz]	T [sec]
0	400	25
10	400	25
50	2000	5
100	4000	2.5
200	8000	1.25

Table 2. Relay Response

f [Hz]	ϕ_{on} [Deg]	ϕ_{off} [Deg]
10	0	0
50	9	18
100	18	28.8
200	21.6	50.4

Table 3. Experiment Variables

f [Hz]	K_L	Tube Length [in]	Pressure [psi]
10	0.346	1	2
50	0.815	10	10
100	1.135	30	50
200	1.454	100	

was compared to the output from the relay. These signals were viewed on an oscilloscope and sampled with the DAQ board. As can be seen in Table 2, the relay did contribute to a phase lag for the response of the system, but the magnitude was not attenuated. The phase angle delay for turning on was less than for turning off.

3 Uncertainty Analysis

The hot film probe was aligned in the calibrator manually. Care was taken to place the probe as closely in the center of the opening as possible and at the exit plane. To assure that the human error in placing the probe was negligible, the probe was removed and replaced in the calibrator facility several times for a low and high pressure. The voltage from the hot film probe was recorded each time. At a set pressure there was no significant difference between trials. The pressure sensor used has a resolution of 0.0001 mm Hg. Atmospheric pressure was read from a barometer with a resolution of 0.1 mm Hg. The calibration data were fit to a 3rd order polynomial and the error between the calibration points and the curve was computed. These errors were kept below 5% of the velocity. The curve fit was often split in 2 or 3 sections to keep error small across the broad range of velocities needed. For high pressure, very large velocities were experienced, but the ability to accu-

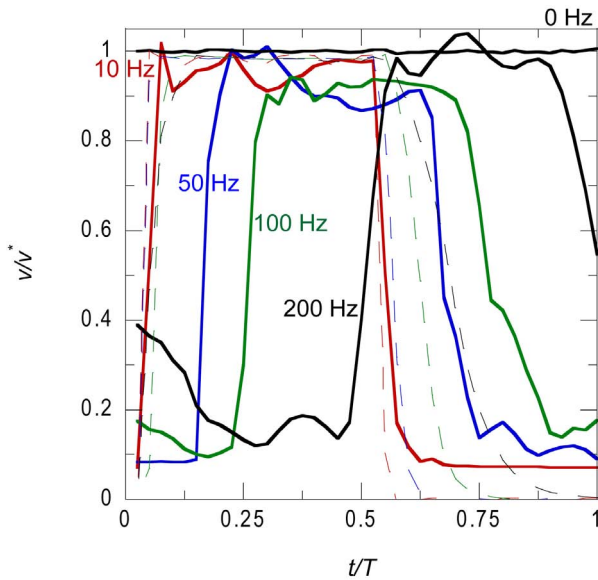


Figure 6. Phase-averaged dimensionless velocity vs. t/T for several frequencies. As frequency increases the phase angle increases and the signal approaches a flat line. The dashed lines are the signal from the solid state relay. A tube length of 3.5 inches, $K_L = 0.815$, and an input pressure of 2 psig was used.

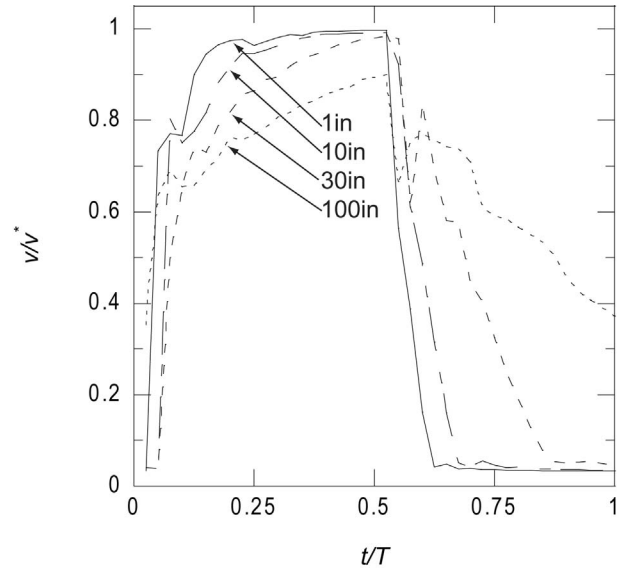


Figure 7. Phase-averaged dimensionless velocity vs. t/T for several lengths. An increase in tube length increases the capacitance of the system, which causes the signal to flatten out. A minor loss of 1.135, an input pressure of 10 psi, and frequency of 10 Hz was used.

rately report low velocities was still required because the valve was shut for part of the cycle.

To collect data the probe was again aligned manually, but a traverse was available to make placing the probe right at the exit plane much easier and more accurate. The velocities were then phase averaged to produce one characteristic period. The precision uncertainty for each point on the wave is given by $1.96 * \sigma / \sqrt{N}$ with 95% confidence, where σ is the standard deviation of the phase-averaged data. Precision uncertainty was kept within 5% of the mean by increasing N to 10,000 for all cases.

4 Results

Examples of how the signal frequency and tube length influence the output velocity waveform are shown in Fig. 6 and Fig. 7. The effect of the magnitude of the minor loss placed before the diffuser is shown in Fig. 8. In each of the plots, v/v^* is the phase-averaged velocity normalized by the mean steady velocity (note that $U = v^*/2$) and t/T is time normalized by the cycle period.

For most flow control applications, including the one of interest here [5], pneumatic control relies on both the

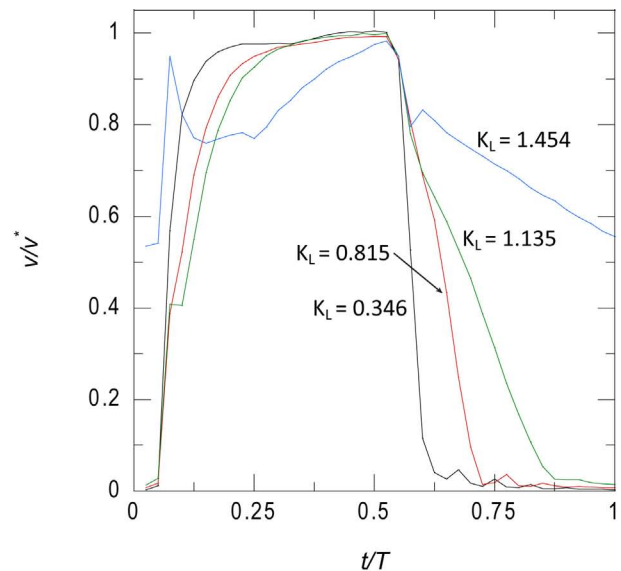


Figure 8. Phase-averaged dimensionless velocity vs. t/T for several minor loss values. The minor loss has a large impact on the magnitude of the response. The loss also contributes to a slow discharge time, which flattens the signal. A tube length of 10 inches, an input pressure of 50 psi, and frequency of 10 Hz was used.

largest and smallest velocity. In other words, achieving a large velocity at the exit is of little use if the velocity does not also reduce to near zero. After trying several other measures of the pulse “robustness,” we have settled on using the standard deviation of the velocity signal as a measure, since it is sensitive to both the maximum and minimum velocity. The standard deviation of the velocity signal is used to help measure how close to a square wave the velocity signal was. If the velocity fails to return to a zero velocity between pulses, or if the peak velocity is attenuated, the standard deviation decreases.

The standard deviations of the velocities are normalized by half the steady flow (0 Hz, corresponding to when the valve is open) value since the standard deviation for a square wave with a duty cycle of 50% that goes from 0 to A is $A/2$. By normalizing the standard deviation of the phase-averaged velocity (U) by half the steady flow velocity in the same system (U_0), a perfect square wave output will result in a value of unity while steady flow would result in 0. Therefore, in general, $0 < U/U_0 < 1$.

Data were first acquired with no minor loss and a 1-inch tube to examine the response of the valve. The data are shown in Fig. 9. The manufacturer specifies the nominal time for the valve to open and close as 1.9 ms and 1.7 ms respectively. Given these values and backed by earlier experiments, the cutoff frequency for the valve is about 278 Hz. The on and off times do produce phase lag, but it is about the same on both ends. For low pressure, the system was more sensitive to frequency. As pressure is reduced, the capacitance is increased, which causes lower frequencies to be attenuated more.

Measurements were made for all 240 combinations of variables. The velocity response data for all cases are shown below in Fig. 10, Fig. 11, Fig. 12, and Fig. 13 for tubes of 3.5, 10, 50, 30 and 100 inches, respectively. The standard deviation of the velocity normalized by the steady flow value divided by 2, U/U_0 , is graphed along the y axis. This represents the standard deviation of the velocity normalized by the standard deviation of a square wave with an amplitude equal to the steady flow velocity through the same system. The response generally drops off with frequency as expected, although, in some cases, it increases. This is especially true for the longer tubes which have resonant frequencies in the range of the excitation frequencies. Generally, as the frequency increases, the pulses becomes less distinct until it deteriorates to a steady state velocity.

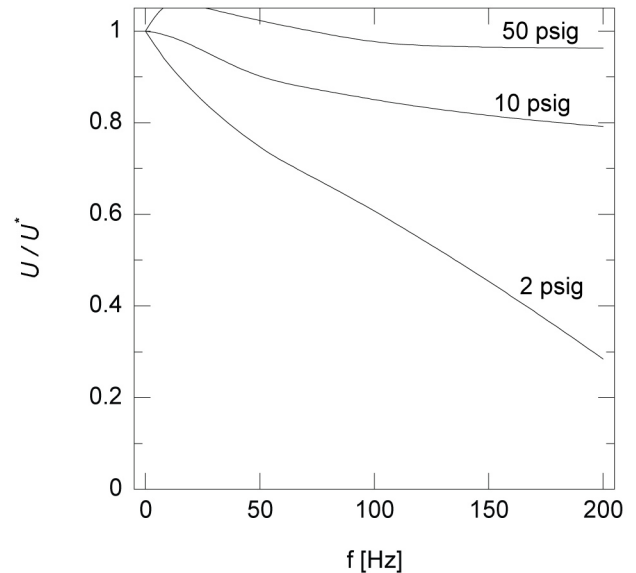


Figure 9. The frequency response for a system with no minor loss and minimal tubing.

Any value reported below about 0.6 is deemed not useful for control.

Some other trends are noted:

1. While a larger input pressure results in larger velocity at the exit for steady flow, larger pressures result in reduced performance for pulsed flow.
2. This becomes more true for longer tubes. For the longest tube studied here, a 50 psig supply case could not be successfully pulsed even at 10 Hz.
3. The minor loss has a similar effect as the tube length.

5 Transmission Matrix Model

Flow through a solenoid valve introduces oscillations to the mean flow. Such steady-oscillatory flow in a piping system can be analyzed either in the time domain or in the frequency domain. The transfer matrix method has been an effective tool to determine the frequency response of piping system [6]. The present piping system, illustrated at Fig. 14, consists of duct (pipe) and orifice. The transfer matrix (TM) representation can be deduced once the TM of each component is derived. Since this model assumes incompressible flow, the model will be compared to only the smallest inlet pressure data.

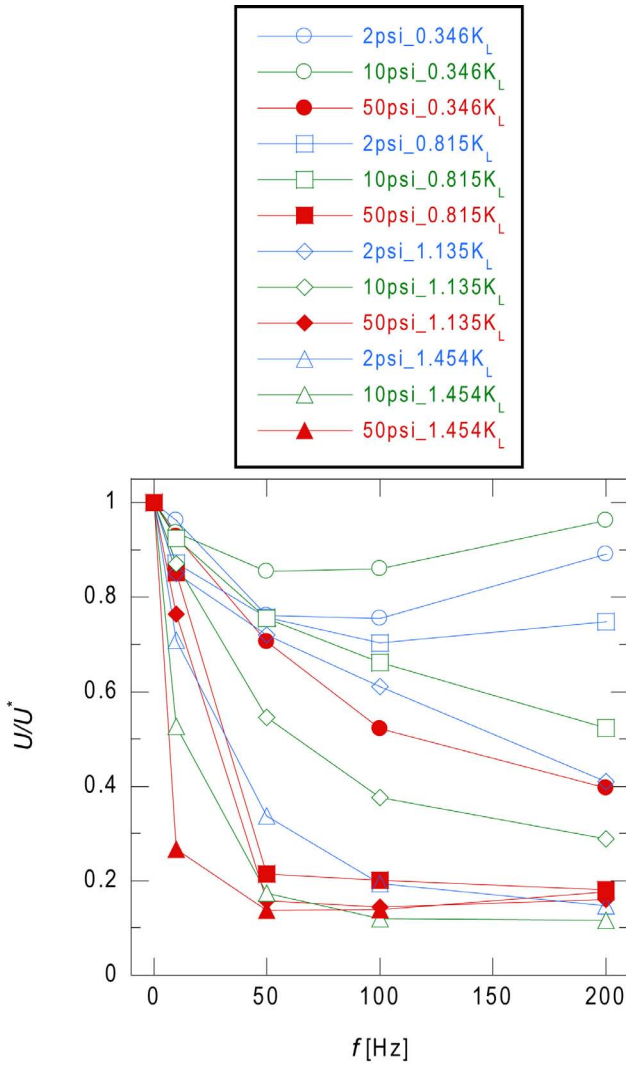


Figure 10. Normalized standard deviation for 3.5-inch length.

5.1 Duct

The TM of duct component, such as pipe 1, 2, 3 and 4 in Fig. 14, is given by [7] as

$$\begin{bmatrix} p' \\ u' \end{bmatrix}_{\text{pout}} = e^{jMk_c L} \begin{bmatrix} \cos(k_c L) & -j\rho_0 c_0 \eta \sin(k_c L) \\ \frac{-j}{\rho_0 c_0 \eta} \sin(k_c L) & \cos(k_c L) \end{bmatrix} \begin{bmatrix} p' \\ u' \end{bmatrix}_{\text{pin}} \quad (2)$$

where L is the length of the pipe, $M = U/c_0 \ll 1$ is the Mach number of mean flow, $()'$ denotes the perturbation of the mean flow at the entrance and exit of the pipe, which

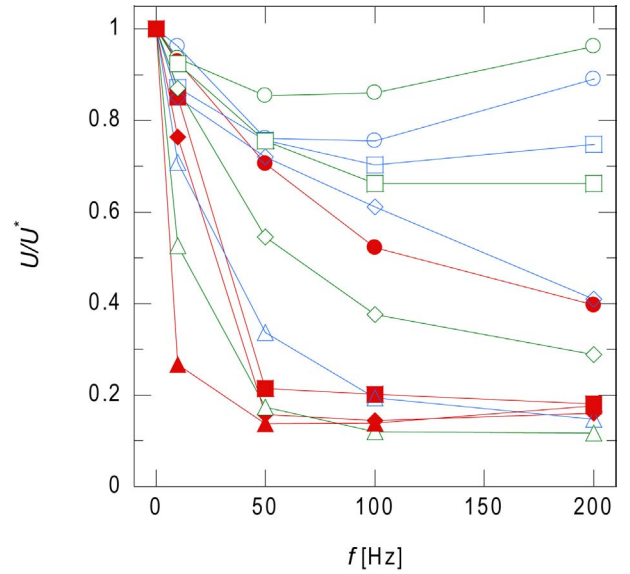


Figure 11. Normalized standard deviation for 10-inch length. Legend shown in Fig. 10.

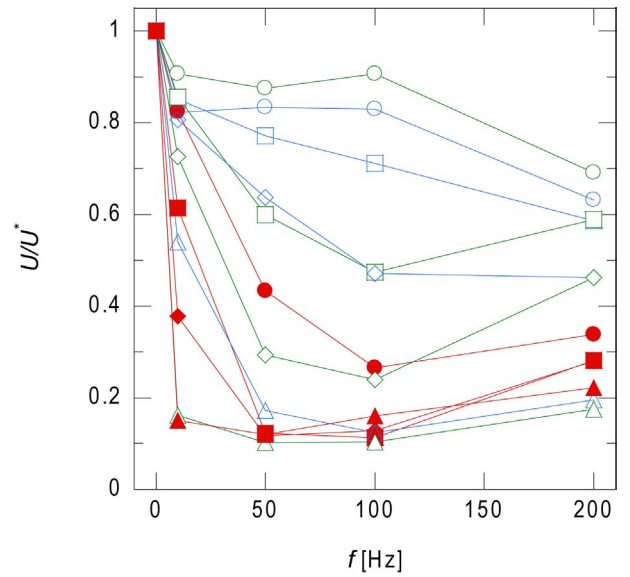


Figure 12. Normalized standard deviation for 30-inch length. Legend is shown in Fig. 10.

is assumed to be small in comparison with its mean flow counterparts. The air density and isentropic speed of sound in air are denoted ρ_0 and c_0 respectively, and

$$\eta \doteq 1 + \frac{\alpha + \zeta M}{k_0} - j \frac{\alpha + \zeta M}{k_0}$$

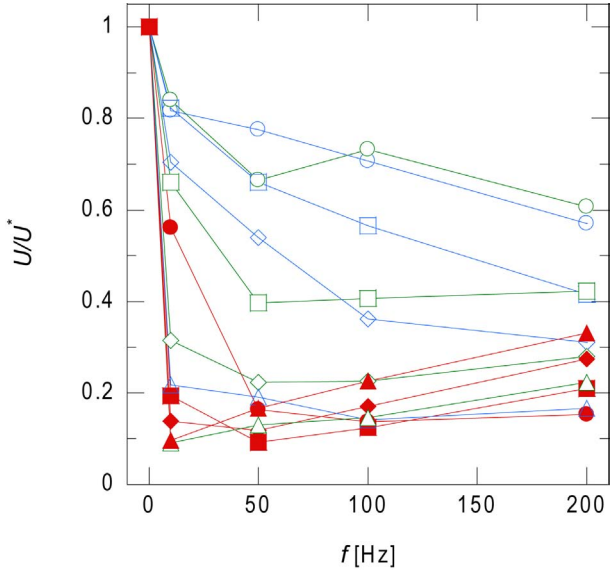


Figure 13. Normalized standard deviation for 100-inch length. Legend is shown in Fig. 10.

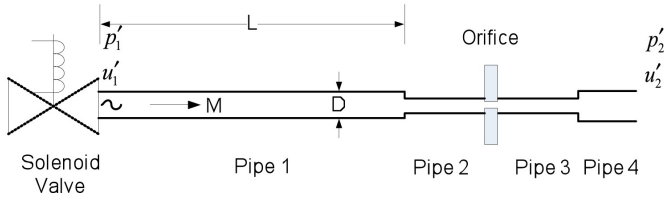


Figure 14. Illustration of a piping system used for the TM model.

$$k_c = [k_0 - j(\alpha + \zeta M)] / (1 - M^2). \quad (3)$$

The coefficients α and ζ account for the visco-thermal loss, and are given by

$$\alpha = \frac{1}{a} \sqrt{\frac{\omega \mu}{2\rho_0 c_0^2}} \left(1 + \frac{\gamma - 1}{\sqrt{Pr}}\right). \quad (4)$$

and

$$\zeta = \psi / 2D, \quad (5)$$

where Pr is the Prandtl number, $2a = D$ is the hydraulic diameter of the pipe, γ is the ratio of specific heats, $\psi =$

$4\bar{\tau}_w / (1/2\rho_0 U^2)$ is the pipe friction factor (assumed to have a value of 0.0072), $\bar{\tau}_w$ is the average wall shear stress, and $\omega = k_0 C$ is the angular frequency of the oscillation. The solenoid valve is excited by a non-sinusoidal periodic signal, in this case a pulse. For this reason, the periodic oscillation is decomposed into Fourier series (harmonics), and the system response is the summation of the response to each harmonic.

5.2 Orifice

The TM of an orifice is given by [8] as

$$\begin{bmatrix} p' \\ u' \end{bmatrix}_{\text{Out}} = \begin{bmatrix} 1 - \rho_0 c_0 M K_L \\ 0 & 1 \end{bmatrix} \begin{bmatrix} p' \\ u' \end{bmatrix}_{\text{Oin}} \quad (6)$$

where the coefficient K_L represents the combination of the effect of the geometry and the vena contracta of the orifice. The coefficient K depends on the orifice geometry and orifice Reynolds number. Typical values of coefficient K as function of Reynolds number are published in [9].

Hence, the TM of the piping system shown in Fig. 14 is

$$\begin{bmatrix} p_2' \\ u_2' \end{bmatrix} = \begin{bmatrix} \text{TM}_{\text{pipe4}} & \text{TM}_{\text{pipe3}} & \text{TM}_{\text{orifice}} \\ \text{TM}_{\text{pipe2}} & \text{TM}_{\text{pipe1}} & \begin{bmatrix} p_1' \\ u_1' \end{bmatrix} \end{bmatrix} \quad (7)$$

Moreover, because the exit of the piping system is an unflanged open-end of a duct of radius r_0 with a flow of Mach number M , the radiation flow impedance of the orifice is given by [10, 11, 12],

$$\begin{aligned} \frac{p_2'}{u_2'} &= Z_r(M) = R_r(M) + jX_r(M) \\ R_r(M) &\approx R_r(0) - 1.1M\rho_0 c_0 \\ X_r(M) &\approx X_r(0) \\ Z_r(0) &= R_r(0) + jX_r(0) = \rho_0 c_0 \frac{1 + \Re}{1 - \Re} \end{aligned} \quad (8)$$

where the reflection coefficient \Re at the orifice is

$$\begin{aligned} \Re &= |\Re| e^{j(\pi - 2k_0 \delta)}, \\ |\Re| &\approx 1 + 0.01336k_0 r_0 - 0.59079(k_0 r_0)^2 \\ &\quad + 0.33756(k_0 r_0)^3 - 0.06432(k_0 r_0)^4 \end{aligned}$$

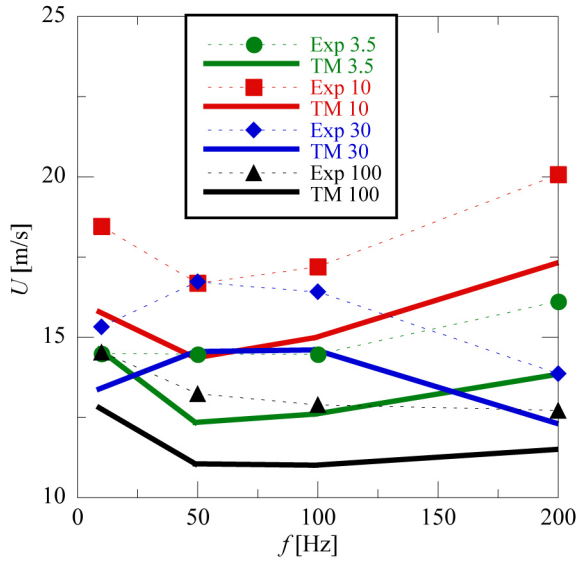


Figure 15. Comparison between the TM prediction and experimental data for the standard deviation of velocity at the exit for $K_L = 0.346$

for $k_0 r_0 \leq 1.5$, where δ is the end correction which is given by

$$\delta = \begin{cases} [0.6133 - 0.1168(k_0 r_0)^2] r_0 & k_0 r_0 \leq 0.5 \\ [0.6393 - 0.1104 k_0 r_0] r_0 & 0.5 < k_0 r_0 < 2. \end{cases}$$

Thus, from Eq. (7) and (8), once one of variables (p'_1 , u'_1 , p'_2 , and u'_2) is known, other variables can be resolved. For all cases, the pressure after the solenoid valve and mean flow velocity at the exit are known. Figure 15 and 16 show the comparison between the TM prediction and experimental data for the velocity (rms) at the exit with different length of pipe 1 and $K_L = 0.346$ and 1.135, respectively. The results show the TM predictions match the trends and are near the magnitude of the experimental data, with the exception of low frequencies for the larger loss.

CONCLUSIONS

Experiments on the response of a pneumatic system consisting of a pressure source, a solenoid valve, and a minor loss, have been presented. As expected, it was found that the response of the system decays with increases in the tube length, the minor loss, and the frequency. A transfer

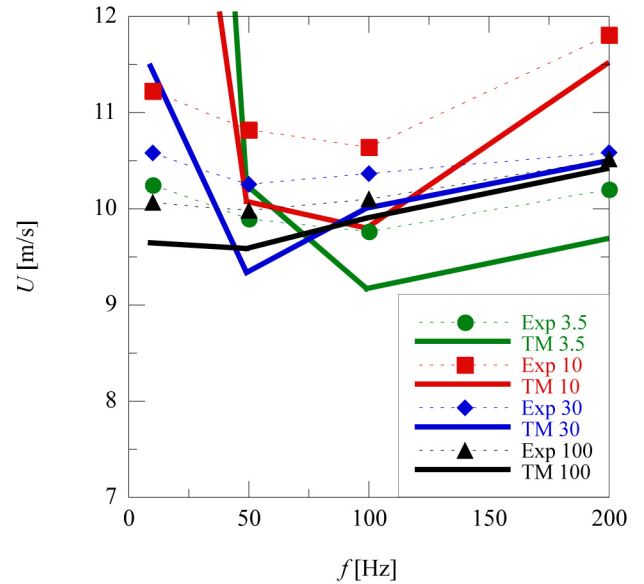


Figure 16. Comparison between the TM prediction and experimental data for the standard deviation of velocity at the exit for $K_L = 1.135$

matrix model was compared with the data for one case, and it was found that the model predicts the same trends with frequency and similar velocity fluctuations as found in the experiments.

REFERENCES

- [1] V. Szente and J. Vad. A semi-empirical model for characterisation of flow coefficient for pneumatic solenoid valves. *Periodica Polytechnica Ser. Eng.*, 47:131–142, 2003.
- [2] C. Braud, A. Dymont, J. Kostas, J. M. Foucaut, and M. Stanislas. Analysis and modelling of a fluidic actuator. ASME Fluids Engineering Conference, 2008. Paper FEDSM2008-55027.
- [3] G. W. Swift. *Thermoacoustics: A unifying perspective for some engines and refrigerators*. Acoustical Society of America, 2002.
- [4] Y. A. Cengel and J. M. Cimbala. *Fluid Mechanics, Fundamentals and Applications*. McGraw Hill, 1st edition, 2006.
- [5] D. Allen and B. L. Smith. Axisymmetric Coanda-assisted vectoring. *Exp. Fluids*, 46(1):55–64, JAN 2009.
- [6] M. H. Chaudhry. *Applied Hydraulic Transients*. Van

Nostrand Reinhold Company, New York, 1979.

- [7] M. L. Munjal. *Acoustics of ducts and mufflers with application to exhaust and ventilation system design*. Wiley-Interscience, New York, 1987.
- [8] C. C. J. Hofmans, R. J. J. Boot, P. O. J. M. Durrieu, and Y. Auregan. Aeroacoustic response of a slit-shaped diaphragm in a pipe at low Helmholtz number, 1: quasi-steady results. *Journal of Sound and Vibration*, 244(1), 2001.
- [9] International standards organization, measurement of fluid flow by means of orifice plates and venturi tubes inserted in circular cross section conduits running full. Technical report, ISO, 1980. ISO 5167-1980.
- [10] H. Levin and J. Schwinger. On the radiation of sound from an unflanged circular pipe. *J. Phys. Rev.*, 73, 1948.
- [11] P. O. A. L. Davies, J. L. Bento Coelho, and M. J. Bhattacharya. Reflection coefficient for an unflanged pipe with flow. *J. Sound and Vibration*, 72, 1980.
- [12] F. P. Mechel. *Formulas of Acoustics*. Springer, New York, 2002.